

1 **Title:** Multiplex Target-Redundant RT-LAMP for Robust Detection of SARS-CoV-2 Using Fluorescent  
2 Universal Displacement Probes

3 **Authors:** Enos C Kline<sup>1</sup>, Nuttada Panpradist<sup>1,2</sup>, Ian T Hull<sup>1</sup>, Qin Wang<sup>1</sup>, Amy K Oreskovic<sup>1</sup>, Peter D  
4 Han<sup>3,4</sup>, Lea M Starita<sup>3,4</sup>, Barry R Lutz<sup>1,4</sup>

### 5 **Affiliations**

6 1 Department of Bioengineering, University of Washington, Seattle, WA, USA

7 2 Global Health for Women Adolescents and Children, School of Public Health, University of  
8 Washington, Seattle, WA, USA

9 3 Department of Genome Sciences, University of Washington, Seattle, WA, USA

10 4 Brotman Baty Institute for Precision Medicine, Seattle, WA, USA

11

12 \* **Correspondence:** B. R. L. (blutz@uw.edu)

13 3720 15<sup>th</sup> Ave NE, Campus Box 355061, Seattle, Washington, United States 98195

14

### 15 **Abstract**

16 The increasing prevalence of variant lineages during the COVID-19 pandemic has the potential to  
17 disrupt molecular diagnostics due to mismatches between primers and variant templates. Point-of-care  
18 molecular diagnostics, which often lack the complete functionality of their high throughput laboratory  
19 counterparts, are particularly susceptible to this type of disruption, which can result in false negative  
20 results. To address this challenge, we have developed a robust Loop Mediated Isothermal Amplification  
21 assay with single tube multiplexed multi-target redundancy and an internal amplification control. A  
22 convenient and cost-effective target specific fluorescence detection system allows amplifications to be  
23 grouped by signal using adaptable probes for pooled reporting of SARS-COV-2 target amplifications or  
24 differentiation of the Internal Amplification Control. Over the course of the pandemic, primer coverage of  
25 viral lineages by the three redundant sub-assays has varied from assay to assay as they have diverged  
26 from the Wuhan-Hu-1 isolate sequence, but aggregate coverage has remained high for all variant  
27 sequences analyzed, with a minimum of 97.4% (Variant of Interest: Eta). In three instances (Delta,  
28 Gamma, Eta), a high frequency mismatch with one of the three sub-assays was observed, but overall  
29 coverage remained high due to multi-target redundancy. When challenged with extracted human samples  
30 the multiplexed assay showed 100% sensitivity for samples containing greater than 30 copies of viral  
31 RNA per reaction, and 100% specificity. These results are further evidence that conventional laboratory  
32 methodologies can be leveraged at the point-of-care for robust performance and diagnostic stability over  
33 time.

### 34 **Introduction**

35 The COVID-19 pandemic is an unprecedented crisis in the modern era, spreading across the  
36 planet in a matter of months, infecting and killing millions, while disrupting the lives of billions (1). An  
37 essential element of the response strategies to COVID-19 is diagnostic testing, which informs clinical  
38 intervention, quarantine, and epidemiological monitoring (2). Nucleic acid amplification tests (NAATs)

39 remain the most accurate approach for diagnosis of infectious diseases including SARS-CoV-2 infection.  
40 However, RNA viruses like SARS-CoV-2 have a high mutational rate, which can result in elevated levels  
41 of sequence diversity accumulating as they propagate. This is a critical obstacle for NAATS because  
42 mismatches between the primer oligonucleotides and the template sequences can impair an assay and  
43 produce false negative results. As transmission has progressed, SARS-CoV-2 has diversified in distinct  
44 lineages, each with signature mutations throughout the genome (3). The emergence of this genetic  
45 diversity has rendered some NAATs susceptible to false negative results, causing these tests to be altered  
46 or withdrawn by the U.S. FDA (4). This challenge posed by mutation for NAATs is not limited to SARS-  
47 CoV-2; similar phenomena have been observed for other human pathogens (5, 6).

48 Laboratory testing strategies to lessen this risk include redundant testing with alternative  
49 methods, diagnostic panels with multiple target regions (7), and/or primer sets with degenerate bases to  
50 account for known genetic variability (8). While degenerate primers are accessible and inexpensive, they  
51 are often limited by assay design constraints and do not account for unknown or novel mutations. Repeat  
52 and multiple testing is an effective strategy, but requires additional resources, labor, and complexity of  
53 design or implementation. These considerations are manageable in contemporary diagnostic laboratories  
54 but can be prohibitive in lower resource settings. Nearly all laboratory assays for SARS-CoV-2 use  
55 redundant targets to mitigate mutations and an internal control to account for sample processing or  
56 interference.

57 A critical aspect of the Center for Disease Control and Prevention's (CDC) Strategy for Global  
58 Response to COVID-19 (2020-2023) is augmenting our current ability to rapidly identify COVID-19  
59 infections so that the chain of transmission can be disrupted. Essential to this effort is the development of  
60 diagnostics that can be performed at the point-of-care (POC); that minimize the time to result (TTR) of  
61 the test and are deployable in otherwise underserved populations. These settings are inherently "low  
62 resource," and necessitate diagnostic methods with simplified chemistry, hardware, and limited sample  
63 processing relative to the standard of practice for molecular diagnostics, polymerase chain reaction  
64 (PCR). Advancements in isothermal nucleic acid amplification technologies over the past three decades  
65 largely satisfy these constraints while still providing high sensitivity. This has led to a boom in isothermal  
66 amplification technologies and NAATs based on them (9). Despite their advantages, there are some areas  
67 where the isothermal NAATs are lacking when compared to PCR. Single-pot multiplexing has been  
68 infrequently demonstrated despite being a prerequisite for internal amplification control (IAC) systems  
69 and useful for multiple target redundancy (10–12) In this work we look to contribute to this capability as  
70 it relates to Loop Mediated Isothermal Amplification (LAMP) for the detection of SARS-COV-2.

71 Herein we describe a multiplexed reverse transcriptase LAMP (mRT-LAMP) combining three  
72 assays, each targeting a unique region of the nucleocapsid (NC) gene, and an IAC assay to validate  
73 diagnostic viability with a negative result. To accomplish this, we have designed a universal target  
74 specific fluorescence probe system. In this method, engineered adapter sequences are incorporated into  
75 the LAMP amplicons which then serve as a template for detection by displacement probes. The resulting  
76 assay chemistry is sensitive, specific, and durable while simplifying the development process. We  
77 evaluate the limit of detection, cross-reactivity with other organisms, and reactivity with extracted RNA  
78 from patients infected SARS-CoV-2.

## 79 **Materials and Methods**

### 80 **Preparation of TFPol polymerase**

81 Plasmid preparation and protein expression and purification were performed as previously described (13).

## 82 Primer and IAC design

83 Three sets of LAMP primers (**Table 1**) targeting different regions of the SARS-CoV-2  
 84 nucleocapsid phosphoprotein were designed manually using the primer design feature of Geneious 8.1.9  
 85 (14) against the SARS-CoV-2 reference sequence (GenBank accession number: NC\_045512). IDT  
 86 OligoAnalyzer (15) and NUPACK (16) were used to evaluate designs in silico. Each target design  
 87 consists of the six conventional LAMP primers: F3, B3, FIP, BIP; LF, and LR (17). The IAC was  
 88 designed using a composite primer technique (18) for LAMP. IAC template sequence was derived from  
 89 target region “NC1” by substituting the target loop primer binding sites with engineered sequences. One  
 90 of the engineered IAC loop sites was used as an IAC loop primer while the other was omitted, so that the  
 91 IAC assay uses a single loop primer (LFc mut in **Fig. 1B**). For each primer set a loop primer was  
 92 modified by the addition of an engineered probe adapter sequence at its 5’ end, with all targets sharing a  
 93 common adapter and the control assay using a second unique adapter sequence. Primer oligonucleotides  
 94 were sourced from Integrated DNA Technologies (Coralville, Iowa, USA).

95 **Table 1: Primer, Probe, and control sequences for the SARS-CoV-2 mRT-LAMP.** For Primers and  
 96 probes, F2/B2 sequences are underlined, non-template linker sequences are italicized, and adapter  
 97 sequences are shown in bold.

SARS-CoV-2 NC1 Primers	Sequence
NC1 FIP	CCACTGCGTTCTCCATTCTTTT <u>CCCCGCATTACGTTTGGT</u>
NC1 BIP	GCGATCAAACAACGTCGGTTATTGCCATGTTGAGTGAGAGCG
NC1 LF	TGGTTACTGCCAGTTGAATCT
NC1 LB + Target adapter	<b>ACCAACACCTCACATCACACATAAT</b> AGGTTTACCCAATAATACTGCGTCTTG
NC1 F3	TGGACCCCAAAATCAGCG
NC1 B3	ATCTGGACTGCTATTGGTGTTA
SARS-CoV-2 NC2 Primers	Sequence
NC2 FIP	CAGCTTCTGGCCCAGTTCTGTGGTGGTGACGGTAAATG
NC2 BIP	CTTCCCTATGGTGCTAACAAAGTCCAATGTGATCTTTTGGTGTATTCA
NC2 LF	GTAGTAGAAATACCATCTTGGACT
NC2 LB + Target adapter	<b>ACCAACACCTCACATCACACATAATA</b> ATATGGGTTGCAACTGAGGGAG
NC2 F3	CTACTACCGAAGAGCTACCAG
NC2 B3	GCAGCATTGTTAGCAGGATTG
SARS-CoV-2 NC3 Primers	Sequence
NC3 FIP	TGTGTAGGTCAACCACGTTCTGCTTCAGCGTTCCTTCGGA
NC3 BIP	GTGCCATCAAATTGGATGACAAAGTTTTGTATGCGTCAATATGCTTATTCA G
NC3 LF + Target adapter	<b>ACCAACACCTCACATCACACATAATA</b> TCCATGCCAATGCGCGACA
NC3 LB	CCAAATTTCAAAGATCAAGTCAT
NC3 F3	GACCAGGAACTAATCAGACAAG
NC3 B3	GCTTGAGTTTCATCAGCCTTC
IAC (NC1) primer	Sequence
IAC FL + Control adapter	<b>ACCACACCTACCACCTAATAACTA</b> ACTCCAGCCATCCTCACCATC
SARS-CoV-2 UDP	Sequence
Target (CoV) UDP Probe	FITC- CCATCAGCACCAAGACTACCCACCTGCCACCAA <b>ACCAACACCTCACATCAC</b> <b>ACATAATA</b>
Target (CoV) UDP Quencher	TTGGTGGCGAGGTGGGTAGTCTTGGTGCTGATGG - Iowa Black® FQ

IAC UDP	Sequence
Control (IAC) UDP Probe	Tex615- CCTGACCACTTCCGAACCCAACCACTACGACAG <b>ACCACACCTACCACCACT</b> <b>AATAACTAA</b>
Control (IAC) UDP Quencher	CTGTCGTAGGTGGTTGGGTTCCGGAAGTGGTCAGG – BHQ®-2
IAC Template	Sequence
IAC ssDNA	AAT GGA CCC CAA AAT CAG CGA AAT GCA CCC CGC ATT ACG TTT GGT GGA CCC TCT GGA GTC AAT GGG TGG TGC CAG AAT GGA GAA CGC AGT GGG GCG CGA TCA AAA CAA CGT CGG CCC CAA GTT GAT CTC CAG CCA TCC TCA CCA TCG TTC ACC GCT CTC ACT CAA CAT GGC AAG AAT TAA CAC CAA TAG CAG TCC AGA TG

98

### 99 **Universal displacement probe design**

100 Two engineered universal displacement probes (UDP) corresponding to the target adapter or IAC  
101 adapter sequence were designed. Each UDP consists of an oligonucleotide duplex with a 3' overhang and  
102 a fluorophore quencher pair (19). The adapter sequence is located at the 3' overhang position, with a  
103 fluorophore spacer sequence at the 5' end and a 5' terminal fluorophore (6-FAM or TEX615). The  
104 quencher (Iowa Black® FQ or Black hole Quencher®-2) sequence is a complementary fluorophore  
105 spacer sequence and is labeled with a 3' dark quencher so that it quenches the fluorophore when annealed.  
106 Probe adapters and universal displacement probe sequences were generated from randomized sequence  
107 and manually modified in Geneious, using OligoAnalyzer and NUPACK as secondary analysis tools, to  
108 minimize dimer and hairpin structures within and between the probes and adapted loop primers. All  
109 designs were tested individually and multiplexed in combination against synthetic dsDNA gBlocks™  
110 (Integrated DNA Technologies, Coralville, Iowa, USA) target and ssDNA IAC Ultramer™ (Integrated  
111 DNA Technologies, Coralville, Iowa, USA) fragments to inform iterative design changes to individual  
112 assays. Final design iterations are reported; probes and quenchers oligonucleotides were sourced from  
113 Integrated DNA Technologies (Coralville, Iowa, USA).

### 114 **Patient samples**

115 A panel of 102 human respiratory specimens was used to evaluate our mLAMP assay  
116 performance. These specimens collected from nasal or nasopharyngeal swabs were suspended in 3mL  
117 viral transport medium (Becton Dickinson 220220), aliquoted, and stored at –80°C until testing as  
118 described (20). The panel was originally characterized by OpenArray (ThermoFisher Scientific, Waltham,  
119 MA, USA) to contain at least 30 COVID-POS across a wide range of concentrations and 30 COVID-  
120 negative samples as well as other samples identified as positive for other respiratory diseases including,  
121 but not limited to, *Streptococcus pneumoniae*, Influenza, seasonal Coronavirus, Adenovirus, and  
122 Enterovirus. **Supplementary Table S1** shows detailed profile in each specimen used in this study.  
123 Samples were reassessed in house for the presence of SARS-CoV-2 RNA, as described below, to account  
124 for losses during freeze-thaws, storage, or extraction. In-house results were used as the reference standard.  
125 Specimens were collected and tested for SARS-CoV-2 infection as part of the Seattle Flu Study, as  
126 approved by the Institutional Review Board at the University of Washington (IRB#: STUDY0006181).  
127 Informed consent was obtained for all participant samples, including for use of de-identified, remnant  
128 specimens.

### 129 **Patient sample preparation**

130 Specimens were extracted using the QIAamp Viral RNA Mini Kit (Qiagen # 52906) according to  
131 the manufacturer's protocol. 100 $\mu$ L of sample was mixed with 40 $\mu$ L negative VTM (to reach the  
132 manufacturer's recommended 140 $\mu$ L input), extracted, and eluted in 70 $\mu$ L buffer. 5 $\mu$ L aliquots were  
133 prepared for single use to avoid free thawing and stored at  $-80^{\circ}\text{C}$  until use.

#### 134 **mRTLAMP protocol**

135 20 $\mu$ L mRT-LAMP reaction contains 5mM DTT, 8 mM magnesium sulfate, 20 mM Tris-HCl, 10  
136 mM ammonium sulfate, 10 mM KCl, 0.5% (v/v) Triton X-100, 1 $\mu$ M of each FIP and BIP primers, 500  
137 nM of each LF and FB primers, 200 nM of each FV and BV primers, 200 nM FAM-tagged UDP probe  
138 and TEX 615 UDP probe, 300 nM Quencher 1 and Quencher 2 probes, 10 units of RNasin® Plus  
139 Ribonuclease Inhibitor (Promega, N2611), 6 units of WarmStart® RTx (NEB, M0380L), 0.7  $\mu$ g Tfpol  
140 polymerase, and 2 units of thermostable inorganic pyrophosphatase (NEB, M0296L). 5 $\mu$ L of extracted  
141 RNA was added to 15 $\mu$ L mLAMP reaction mixture and incubated at  $63.3^{\circ}\text{C}$  for 1 hour. Fluorescence  
142 measurements for FAM and TEX 615 signal, indicating SARS-CoV-2 and IAC amplification,  
143 respectively, were taken every 25 seconds (accounting for 13 second cycle and read times).

#### 144 **RT-PCR protocol**

145 The RT-PCR protocol was prepared as previously described (20). Each 20 $\mu$ L RT-PCR reaction  
146 contains 5mM DTT, 200 $\mu$ M ea. dNTP, 1x of either N1, N2, or RP primer/probe mix (IDT, 10006770),  
147 80mM Tris-sulfate, 20mM ammonium sulfate, 4mM magnesium sulfate, 5% (v/v) glycerol, 5% (v/v)  
148 DMSO, 0.06% (v/v) IGEPAL CA-630, 8.4% (w/v) trehalose, 0.05% (v/v) Tween-20, 0.5% (v/v) Triton X-  
149 100, 7.5U reverse transcriptase (NEB M0380L), and 2.5U polymerase (NEB M0481L). 5 $\mu$ L of extracted  
150 RNA was added to the 15 $\mu$ L RT-PCR reaction mixture and subjected to 5 minutes at  $55^{\circ}\text{C}$ , 1 minutes of  
151  $94^{\circ}\text{C}$  and 45 cycles of 1 second  $94^{\circ}\text{C}$  and 30 seconds at  $57^{\circ}\text{C}$  and read using FAM channel on a CFX96  
152 (Bio-Rad Laboratories, Hercules, California). Each clinical sample was run with one technical replicate  
153 for each N1, N2, or RP assay, along with standards using synthetic RNA templates prepared in-house and  
154 quantified using ddPCR as described (21). Cq and SQ values were exported from Bio-Rad CFX Maestro  
155 1.1 software (version 4.1.2433.1219) using the RFU threshold of 50 across all datasets.

#### 156 **Sequence analysis**

157 Genomic sequences of SARS-COV-2 were downloaded from GISAID.ORG  
158 (**acknowledgements: Supplementary Tables S2-S8**). Criteria for inclusion were: sequences with  
159 designation as a Variant of Concern (VOC) or Variant of Interest (VOI) filtered for completeness, high  
160 coverage, collection on or before June 14, 2021 and submitted prior to July 1, 2021. The first 1000  
161 sequence records for each VOC / VOI in the GISAID.ORG database were used for subsequent analysis.  
162 This sequence library was screened for perfect identity matches with the primer binding regions of the  
163 NC1, NC2, NC3 assays using the packages Biostrings (22) and Seqnr for R (23).

#### 164 **Results**

165 To efficiently combine mRT-LAMP assays and differentiate between target and IAC  
166 amplification in a crude sample matrix requires two key features: a target specific probe technology (**Fig.**  
167 **1**) and a strand displacement polymerase with low non-template amplification. We developed fluorescent  
168 universal displacement probes (**UDPs**) to allow multiplexed assays to be combined or parsed into  
169 fluorescence channels with a minimum number of probes. UDPs themselves are engineered sequences  
170 that use a universal adapter sequence on a loop primer for target-specific detection (**Fig. 1A**). In the  
171 configuration presented here, three independent SARS-CoV-2 targets are designed to report to a single

172 green (6-FAM) fluorescent probe, and the IAC is designed to report to a red (TEX615) fluorescence  
173 channel (**Fig. 1B**). We previously developed an in-house thermostable strand displacement polymerase  
174 (TFpol) with very low nonspecific amplification that is amenable to multiplexing. The TFpol design was  
175 inspired by the chimeric polymerase method of Morant (24) using the polI polymerase of *Thermus*  
176 *Thermophilus* as the backbone, an enzyme shown to be tolerant of many polymerase inhibitors (25, 26).  
177 UDPs and TFpol combine to allow for a flexible and robust mLAMP system, compatible with multiple  
178 target redundancy, IAC controls, and potential for reduced sample preparation.

179

180

181 **Figure 1: Multiplexed RT-LAMP (mRT-LAMP) fluorescence detection by Universal Displacement**  
182 **Probes (UDP).** **A**) UDP incorporation during LAMP amplification and activation by displacement of  
183 quenching strand. Primer and probe refer to loop (**L**), adapter (**A**), and quencher (**Q**), with complementary  
184 sequences denoted with the suffix “c” (e.g., “Lc” is the reverse complement “L”). **B**) Two-channel  
185 fluorescence detection of multiplexed redundant LAMP products (**6-FAM**) and shared-primer IAC  
186 (**TEX615**) by UDPs. Primer designations refer to forward (**F**), backward (**B**), and loop (**L**) using  
187 conventional LAMP terminology.

188

### 189 **Analytical performance of SARS-CoV-2 mRT-LAMP**

190 Functionality of the individual redundant targets in the mRT-LAMP was verified using synthetic  
191 RNA fragments corresponding to NC1, NC2, or NC3 mRT-LAMP assay footprints. All three target  
192 regions generated detectable amplification (**Supp. Fig. S1A**) with similar average reaction times with 200  
193 copies of transcript RNA (NC1: 26.4 min, NC2: 26.3, NC3: 28.7 min; **Supp. Fig. S1B**).

194 The multiplexed assay was evaluated with synthetic target RNA containing all three target  
195 regions in the presence of 105 copies of a single-stranded DNA internal amplification control (**Fig. 2A**).  
196 The amount of IAC was chosen to allow detection of low-copy targets prior to detection of the IAC, in  
197 order to reduce resource competition between target and control amplifications. This timing differential is  
198 possible because of the reduced rate of amplification with a single loop primer in the IAC primer set,  
199 when compared to the target assays with a standard complement of LAMP primers. Input of 200 SARS-  
200 CoV-2 RNA copies (**Fig. 2A, top**) resulted in detection of green fluorescence in about 21 minutes, while  
201 the IAC was not detected. For zero SARS-CoV-2 input copies, there was no target amplification, and the  
202 IAC signal was detected by red fluorescence at about 27.5 minutes (**Fig. 2A, bot**). This behavior is ideal  
203 for a shared-primer IAC strategy, permitting detection of the target organism or, alternatively, validating  
204 the assay chemistry with the control reaction in the absence of target NAs. The analytical sensitivity was  
205 assessed with synthetic RNA target (**Fig. 2B**). All reactions containing target RNA were positive, and all  
206 NTC reactions detected IAC amplification and were negative for target (**Fig. 2A**). Some IAC  
207 amplifications were detected in low copy reactions containing target RNA (**Fig. 2A**), but their presence  
208 did not compromise target detection. The assay detected down to 5 copies per reaction (n=4), and all  
209 reactions had threshold times of 30 minutes or less for both the target and IAC (**Fig. 2C**).

210

211

212 **Figure 2: Analytical performance of mRT-LAMP for SARS-CoV-2.** A) Characteristic amplification  
213 of multiplexed SARS CoV-2 target and internal amplification control (IAC) with real-time fluorescence  
214 detection by universal displacement probes (UDP). Single representative run with 200 copies of synthetic  
215 RNA input or a no template control (NTC). B) Analytical sensitivity of multiplexed SARS-CoV-2 target  
216 and IAC. IAC amplifications (**bottom**) correspond to target amplifications (**top**). Target synthetic RNA  
217 input: 2,000 (n=3), 200 (n=3), 20 (n=3), 10 (n=3), or 5 copies per reaction (n=4); and NTC (n=3). C)  
218 Time to detect signals from SARS-CoV-2 and IAC for reactions from panel B.

219

## 220 **Tolerance to transport media**

221 To evaluate the tolerance of the assay to potential media contaminants, a selection of  
222 commercially available co buffered transport reagents were spiked into reactions with a 25% final  
223 concentration. For a 20 $\mu$ L total reaction volume, 5 $\mu$ L of 1x DMEM (11965-06, Gibco), 1x VTM (BD  
224 220527, Copan), 1x PBS (SH30256.01, GE) or 0.9% sodium chloride (diluted from 5M stock 71386-1L,  
225 Sigma) was added into the mRT-LAMP reactions with final synthetic SARS-CoV-2 RNA of 0, 20, or 200  
226 copies (**Supp. Fig. S2**). Successful SARS-COV-2 amplification was observed for all samples containing  
227 template under all buffer conditions.

## 228 **Performance with extracted clinical specimens**

229 The SARS-CoV-2 mRT-LAMP was evaluated against a collection of pre-extracted patient  
230 specimens. Of the 102 samples evaluated by RT-PCR, 93 were determined to contain human origin  
231 material by positive RNase P (**RP**) results; all samples that were negative for RP were also negative for  
232 SARS-CoV-2 and were considered indeterminate. Of the 93 specimens verified to contain human  
233 material, 60 were found to be negative for SARS-CoV-2, and 30 were found to be positive by both  
234 reference RT-RCR assays. The three remaining samples were positive for SARS-CoV-2 by one reference  
235 RT-PCR assay and negative by the second, resulting in an inconclusive classification. All samples that  
236 were indeterminate or inconclusive by RT-PCR were excluded from analysis. Clinical samples were run  
237 in duplicate mRT-LAMP reactions.

238 The mRT-LAMP was able to detect negatives with 100% specificity in both sets of replicates,  
239 with detection of the IAC but no target signal (**Fig. 3**). Conversely, sensitivity for the two replicates was  
240 90% (27/30) and 87% (26/30), respectively. For samples found to have more than 30 copies / mRT-  
241 LAMP reaction by reference RT-PCR, sensitivity was improved to 100% (21/21) for both replicates. The  
242 OpenArray characterization of the verified samples found 57 of 90 validated samples contained one or  
243 more other respiratory infections; 8 of 9 SARS-CoV-2 positive samples with coinfections were correctly  
244 called as SARS-CoV-2 positive, 48 of 48 SARS-CoV-2 negative samples that were positive for other  
245 pathogens were correctly called as SARS-CoV-2 negative.

246

247

248 **Figure 3: mRT-LAMP amplification of extracted nasal specimens.** Samples confirmed positive or  
249 negative for SARS-CoV-2 and positive for the RNase P human marker by RT-PCR panel (N1, N2, RP)  
250 were amplified by duplicate mRT-LAMP reactions. Detected mRT-LAMP signals for SARS-CoV-2  
251 (CoV) are shown in blue, and IAC signals are shown in orange; replicate pairs are connected by a line  
252 segment. Mean copy number was derived from qPCR results of N1, N1 PCR (see **Supplemental Table**  
253 **S1**).

## 254 **Primer coverage analysis**

255 Individual primer sets had variability in the frequency of perfect primer matches across the  
256 VOC/VOI sequence libraries (**Table 2**). Presence of mismatches does not necessarily preclude assay  
257 functionality and is therefore an underestimate of realized assay coverage. Combined primer coverage,  
258 where one or more primer sets had a perfect match for the target, was high across all variants, with a  
259 minimum 97.4% (for Eta).

260 **Table 2: Coverage of Variant Sequences by individual and multiplexed targets**

	<b>Primer set (% of perfect primer set alignment to 1000 sequences)</b>			
<b>SARS-COV-2 VOC/VOI</b>	<b>NC1 Primers</b>	<b>NC2 Primers</b>	<b>NC3 Primers</b>	<b>multiplex coverage (1+ primer set match)</b>
Alpha	71.8	90.0	79.9	100.0
Beta	96.4	90.4	95.9	100.0
Delta	96.7	96.5	00.0	99.8
Epsilon	94.6	93.7	81.2	99.6
Gamma	00.5	80.7	88.6	98.8
Eta	93.9	00.4	83.7	97.4
Iota	88.0	81.5	92.5	99.9

261

262

263

## 264 **Discussion**

265 This initial validation of a multiplexed reverse transcription LAMP assay is a further step towards  
266 more resilient point-of-care NAAT technologies with convenient implementation and development. The  
267 assay supports robust but basic functionality with competitive sensitivity, speed, and a low complexity  
268 fluorescence detection system. Because VTM has been shown to inhibit conventional PCR strategies (27),  
269 we designed our assay to use our in-house chimeric polymerase, TFPol, which has been proven to be  
270 effective with complex samples containing various transport media. TFPol supports multiplexed LAMP  
271 amplifications which have been infrequently demonstrated. These capabilities, taken together, enable  
272 features that are contemporary in high-throughput laboratory testing but more challenging in point-of-  
273 care diagnostics.

274 Multiplexed LAMP reactions with the ability to differentiate individual products by target  
275 specific probes enable two key aspects of robust NAAT testing: internal amplification controls and  
276 multiple target redundancy. IACs are widely accepted as a means of assuring the sample could detect a  
277 positive result if the target result is negative, by verifying that the reaction chemistry was viable and not  
278 inhibited by sample contaminants or otherwise compromised (28). In the context of LAMP amplification,  
279 internal controls can impair successful target detection; the resource demands of a successful LAMP



280 mean co-amplification of multiple products with varying inputs often lead to the competitive inhibition of  
281 slower assays or lower concentration of target (**Fig. 2B, 2C**). Presumably, this can be attributed to  
282 resource depletion of limiting reagents in the reaction mix. To address this resource competition, we  
283 devised a shared-primer internal control strategy where the performance of the IAC has been intentionally  
284 impaired by using a reduced primer set. The delayed time-to-detection of the IAC can then be further  
285 controlled by adjusting the concentration of control template, ensuring reduced competition with the  
286 target amplification.

287 The single-pot multiple target redundancy is a defining feature of this assay design even with the  
288 grouped reporter signal. Pathogen genetic variability is an important failure mode for nucleic acid  
289 amplification tests; a single nucleotide point mutation (**SNP**) can result in underperformance of a LAMP  
290 (29) or PCR reaction (30). As the COVID-19 pandemic progresses, the virus will continue to accumulate  
291 mutations and diversify, posing a challenge to NAATs used for diagnosis. An alignment of publicly  
292 available SARS-CoV-2 genomes at the time of writing reveals multiple genomes with known mutations  
293 in the primer footprints of the CDC PCR designs and a range of other published assays, suggesting that  
294 mutations are an existential problem (data not shown). The likelihood of these mutations rendering all  
295 three target amplifications ineffective simultaneously is lower than for a single assay. This principle is  
296 often incorporated in commercially available conventional laboratory based NAATs so this capability  
297 represents a convergence of state-of-the-art diagnostic methods and POC diagnostic capabilities. Our own  
298 analysis (**Fig. 2**) found that, since the design of the multiplex assay in early 2020 against the NCBI  
299 reference sequence, the emergence of the many variant lineages had resulted in some high frequency  
300 mismatches in primer binding regions of our targets. While many single nucleotide polymorphisms are  
301 likely to be tolerated by a LAMP reaction, some mutations, such as those located at or near the critical  
302 termini of primers, may interfere with diagnostic performance (31). Variants Delta, Gamma and Eta each  
303 had fixed, or almost fixed allele mutations in primer sets NC3, NC1, and NC2 respectively. When  
304 considered in combination as a multiplex assay, the primers still showed good overall coverage despite  
305 one of the three assays being potentially compromised; this is a clear demonstration of the value that  
306 multitarget redundancy holds for viral diagnostics. In the case of the Delta variant, which currently has  
307 rising incidence (32), a sequence mutation within the NC3 primer set was identified on the reverse  
308 bumper primer (B3, data not shown). This primer could be altered to be inclusive to the delta variant or  
309 redesigned without disruption to the diagnostic, ensuring no lapse in diagnostic coverage over time.

310 In order to fully realize a field ready POC assay additional development is planned. While  
311 preliminary testing suggests that the system is tolerant to inhibitors that might typically interfere with a  
312 direct-to-amplification workflow, in-amplification sample lysis, and testing with human sample matrix  
313 will be necessary. This is particularly important for understanding the role of RNAses on assay  
314 sensitivity. With the current ssDNA IAC design RNA integrity is not assessed by the control system,  
315 which is essential for a fully functional process control. Future iterations will address this by  
316 implementing an encapsidated RNA, such as MS2 coliphage for this purpose. Sampling, storage, and  
317 portable device solutions are already under development (13). These advancements will allow us to  
318 eschew infrastructure requirements that have acted as a bottleneck in current testing efforts, and when  
319 combined with the robust multiplex chemistry presented here, could act as a practical solution for  
320 decentralized testing.

## 321 **Author Contributions**

322 E.K. designed this unique version of LAMP assay and in-house polymerase. E.K., I.T.H., and  
323 Q.W. prepared the in-house polymerase and synthetic RNA targets. N.P. and E.K. performed mRT-  
324 LAMP experiments. N.P. and A.K.O. performed extraction of clinical specimens, RT-qPCR. E.K.

325 performed the analysis of mRT-LAMP and RT-qPCR. P.D.H. and L.M.A. designed the specimens panel  
326 used in this study and characterized these specimens using RT-qPCR and OpenArray. B.R.L. oversaw the  
327 study. All authors contributed to writing this manuscript.

## 328 **Acknowledgments**

329 We thank other project members in the Lutz lab for their feedback: Robert Atkinson, Michael  
330 Roller, Crissa Bennett, Daniel Lyon, and Jack Henry Kotnik. We thank Dr. Syamal Raychaudhuri, Dr.  
331 Frances Chu from Inbios International, and Dr. Gwong-Jen J. Chang for stimulating discussion. We thank  
332 the Seattle Flu Study and the Seattle Coronavirus Assessment Network (SCAN) teams led by Principal  
333 Investigators: Helen Y. Chu, MD, MPH, Michael Boeckh, MD, PhD, Janet A. Englund, MD, Michael  
334 Famulare, PhD, Barry R. Lutz, PhD, Deborah A. Nickerson, PhD, Mark J. Rieder, PhD, Lea M. Starita,  
335 PhD, Matthew Thompson, MD, MPH, DPhil, Jay Shendure, MD, PhD and Trevor Bedford, PhD for  
336 providing specimens for testing. This work was supported by the Seattle Flu Study (funded by Gates  
337 Ventures) and the National Institutes of Health (R01AI140845; 5R61AI140460-03). I.T.H. was supported  
338 in part by the National Institute of General Medical Sciences of the National Institutes of Health under  
339 Award Number T32GM008268. This work does not reflect the views of the funders. The funders were  
340 not involved in the design of the study, and funders do not have any ownership over the management and  
341 conduct of the study, the data, or the rights to publish.

## 342 **Conflicts of Interest**

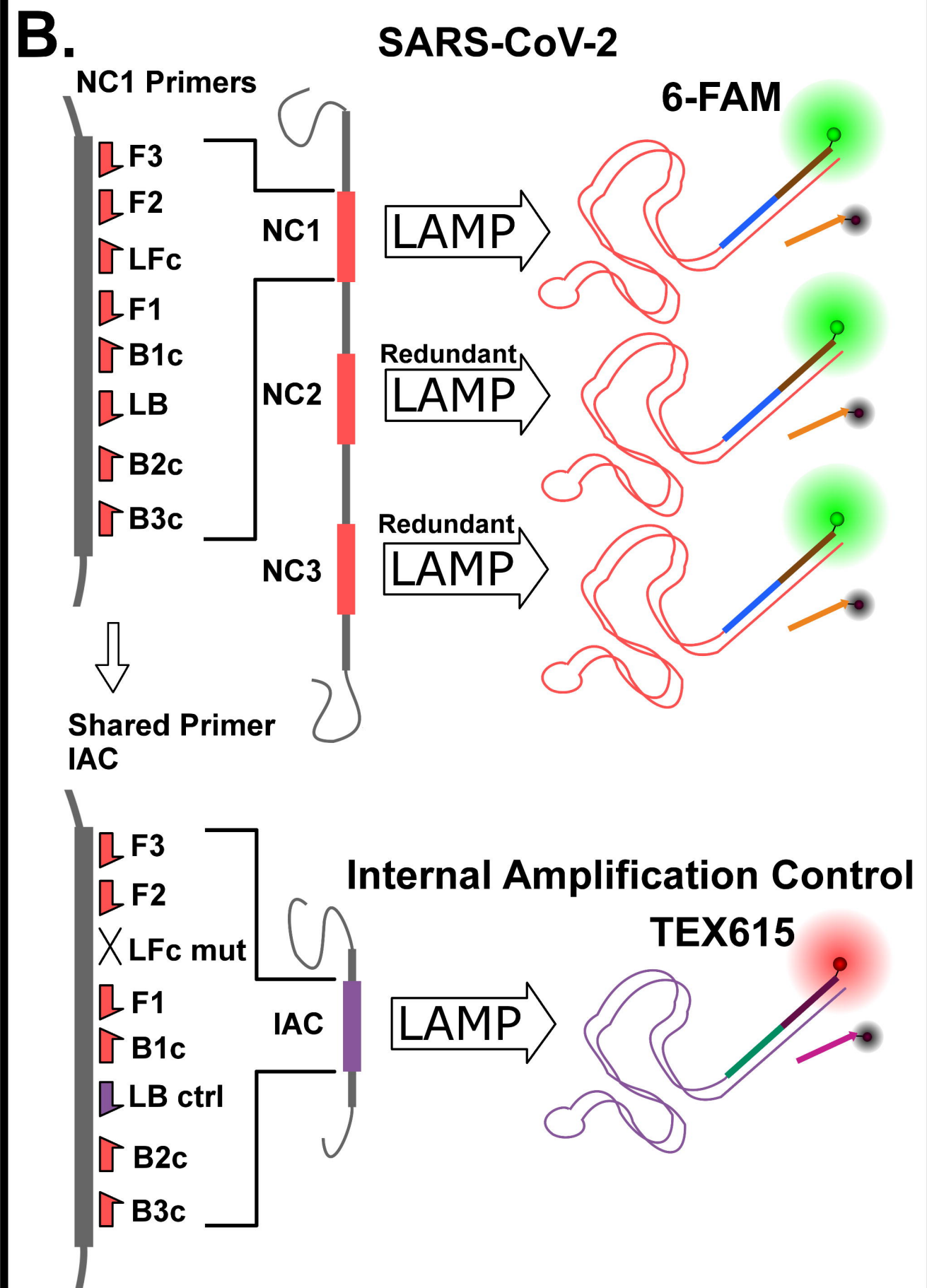
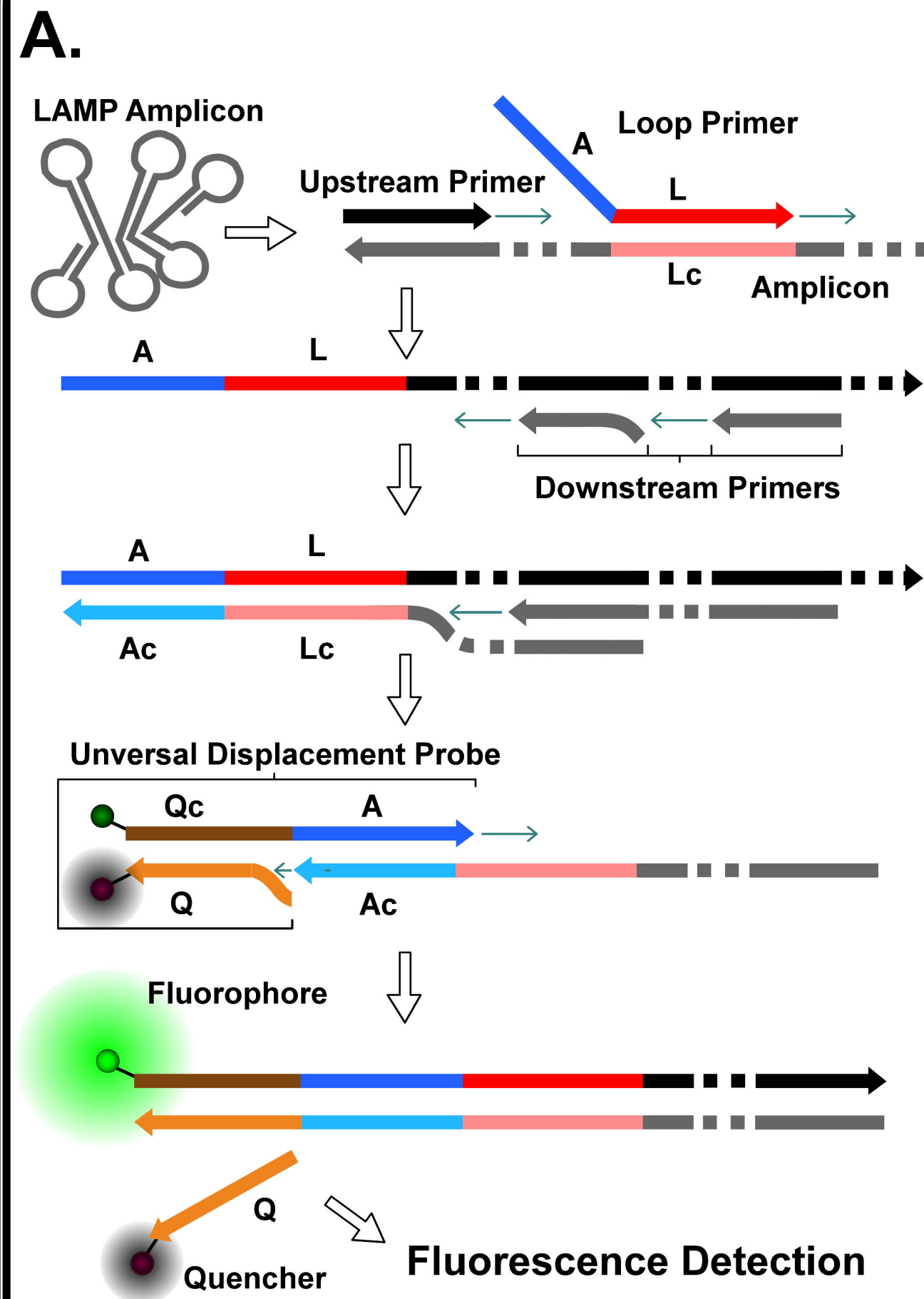
343 Patent applications have been filed on several components of this assay. E.C.K., N.P., Q.W.,  
344 I.T.H., D.L. and B.R.L. are inventors on one or more provisional patent applications. E.C.K., N.P., Q.W.,  
345 I.T.H., A.K.O, and B.R.L. have equity in a startup company that licenses this technology.

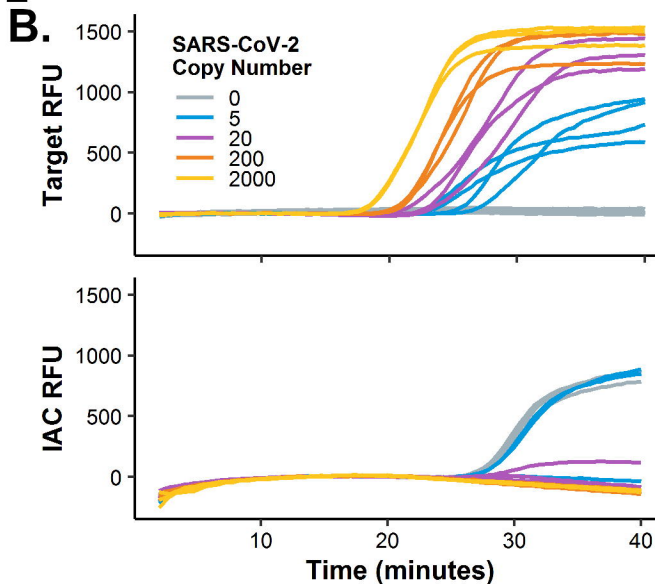
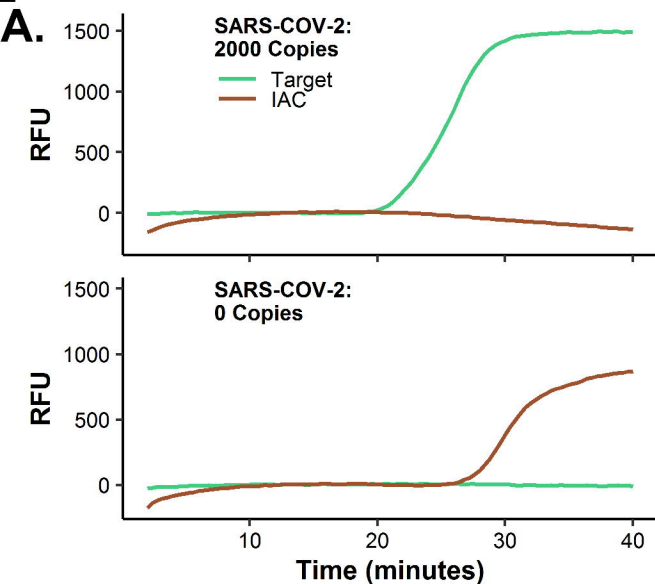
## 346 **References**

- 347 1. Ghebreyesus TA. 2020. WHO Director-General's opening remarks at the media briefing on  
348 COVID-19 - 11 March 2020.
- 349 2. Centers for Disease Control and Prevention. 2021. CDC Strategy for Global Response to  
350 COVID-19 (2020-2023).
- 351 3. Rambaut A, Holmes EC, O'Toole Á, Hill V, McCrone JT, Ruis C, Plessis L du, Pybus OG. 2020.  
352 A dynamic nomenclature proposal for SARS-CoV-2 lineages to assist genomic epidemiology.  
353 *Nat Microbiol* 5:1407.
- 354 4. United States Food and Drug Administration. 2021. Genetic Variants of SARS-CoV-2 May Lead  
355 to False Negative Results with Molecular Tests for Detection of SARS-CoV-2 - Letter to Clinical  
356 Laboratory Staff and Health Care Providers.
- 357 5. Stellrecht KA. 2018. The Drift in Molecular Testing for Influenza: Mutations Affecting Assay  
358 Performance. *J Clin Microbiol* 56:e01531-17.
- 359 6. Ison CA, Golparian D, Saunders P, Chisholm S, Unemo M. 2013. Evolution of *Neisseria*  
360 *gonorrhoeae* is a continuing challenge for molecular detection of gonorrhoea: false negative  
361 gonococcal porA mutants are spreading internationally. *Sex Transm Infect* 89:197–201.
- 362 7. Peñarrubia L, Ruiz M, Porco R, Rao SN, Juanola-Falgarona M, Manissero D, López-Fontanals  
363 M, Pareja J. 2020. Multiple assays in a real-time RT-PCR SARS-CoV-2 panel can mitigate the

- 364 risk of loss of sensitivity by new genomic variants during the COVID-19 outbreak. *Int J Infect*  
365 *Dis* 97:229.
- 366 8. World Health Organization. 2021. WHO information for the molecular detection of influenza  
367 viruses.
- 368 9. Obande GA, Singh KKB. 2020. Current and Future Perspectives on Isothermal Nucleic Acid  
369 Amplification Technologies for Diagnosing Infections. *Infect Drug Resist* 13:483.
- 370 10. Tanner NA, Zhang Y, Evans TCJ. 2012. Simultaneous multiple target detection in real-time loop-  
371 mediated isothermal amplification. *Biotechniques* 53:81–89.
- 372 11. Ding S, Chen G, Wei Y, Dong J, Du F, Cui X, Huang X, Tang Z. 2021. Sequence-specific and  
373 multiplex detection of COVID-19 virus (SARS-CoV-2) using proofreading enzyme-mediated  
374 probe cleavage coupled with isothermal amplification. *Biosens Bioelectron* 178:113041.
- 375 12. Bhadra S, Riedel TE, Lakhotia S, Tran ND, Ellington AD. 2021. High-Surety Isothermal  
376 Amplification and Detection of SARS-CoV-2. *mSphere* 6:e00911–e00920.
- 377 13. Panpradist N, Kline E, Atkinson RG, Roller M, Wang Q, Hull IT, Kotnik JH, Oreskovic AK,  
378 Bennett C, Leon D, Lyon V, Gilligan-Steinberg S, Han PD, Drain PK, Starita LM, Thompson  
379 MJ, Lutz BR. 2021. Harmony COVID-19: a ready-to-use kit, low-cost detector, and smartphone  
380 app for point-of-care SARS-CoV-2 RNA detection. medRxiv.
- 381 14. Rozen S, Skaletsky H. 2000. Primer3 on the WWW for General Users and for Biologist  
382 Programmers. *Methods Mol Biol* 132:365–386.
- 383 15. Integrated DNA Technologies. 2020. OligoAnalyzer™ Tool. Coralville, Iowa.
- 384 16. Zadeh JN, Steenberg CD, Bois JS, Wolfe BR, Pierce MB, Khan AR, Dirks RM, Pierce NA. 2011.  
385 NUPACK: Analysis and design of nucleic acid systems. *J Comput Chem* 32:170–173.
- 386 17. Nagamine K, Hase T, Notomi T. 2002. Accelerated reaction by loop-mediated isothermal  
387 amplification using loop primers. *Mol Cell Probes* 16:223–229.
- 388 18. Hoorfar J, Malorny B, Abdulmawjood A, Cook N, Wagner M, Fach P. 2004. Practical  
389 Considerations in Design of Internal Amplification Controls for Diagnostic PCR Assays. *J Clin*  
390 *Microbiol* 42:1863–1868.
- 391 19. Faltin B, Zengerle R, von Stetten F. 2013. Current Methods for Fluorescence-Based Universal  
392 Sequence-Dependent Detection of Nucleic Acids in Homogenous Assays and Clinical  
393 Applications. *Clin Chem* 59:1567–1582.
- 394 20. Panpradist N, Wang Q, Ruth PS, Kotnik JH, Oreskovic AK, Miller A, Stewart SWA, Vrana J,  
395 Han PD, Beck IA, Starita LM, Frenkel LM, Lutz BR. 2021. Simpler and faster Covid-19 testing:  
396 Strategies to streamline SARS-CoV-2 molecular assays. *EBioMedicine* 64:103236.
- 397 21. Gulati GK, Panpradist N, Stewart SW, Beck IA, Boyce C, Oreskovic AK, Avila-Ríos S, Han PD,  
398 Reyes-Terán G, Starita L, Frenkel LM, Lutz BR, Lai JJ. 2021. Inexpensive workflow to enable  
399 simultaneous monitoring HIV viral load and detection of SARS-CoV-2 infection. medRxiv.
- 400 22. Pagès H, Aboyou P, Gentleman R, DebRoy S. 2021. Biostings: Efficient manipulation of  
401 biological strings. 2.60.2. Bioconductor.

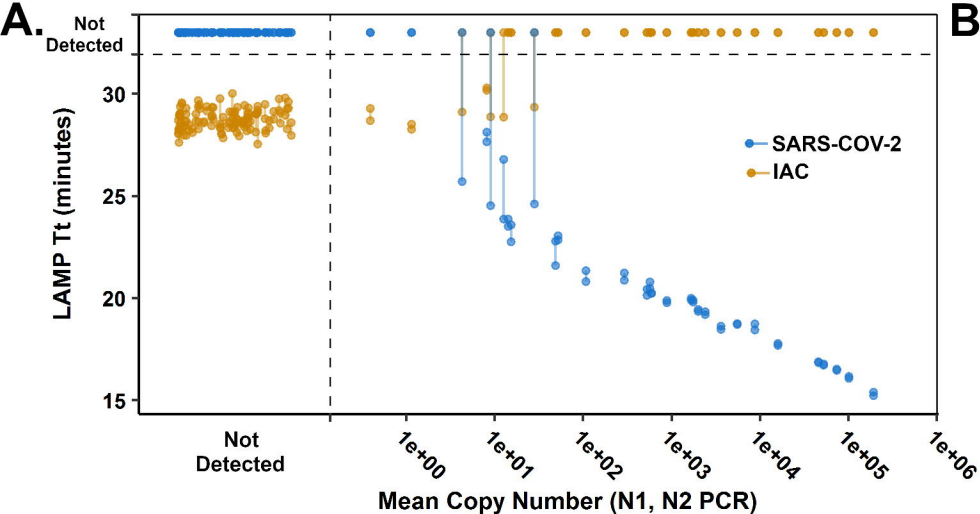
- 402 23. Charif D, Lobry JR. 2007. SeqinR 1.0-2: A Contributed Package to the R Project for Statistical  
403 Computing Devoted to Biological Sequences Retrieval and Analysis, p. 207–232. In Bastolla, U,  
404 Porto, M, Roman, H, Vendruscolo, M (eds.), Structural Approaches to Sequence Evolution.  
405 Springer, Berlin, Heidelberg.
- 406 24. Morant N. 2015. Novel thermostable DNA Polymerases for isothermal DNA amplification.  
407 University of Bath, Bath, United Kingdom.
- 408 25. Poddar S, Sawyer M, Connor J. 1998. Effect of Inhibitors in Clinical Specimens on Taq and Tth  
409 Dna Polymerase-Based Pcr Amplification of Influenza A Virus. *J Med Microbiol* 47:1131–1135.
- 410 26. Abu Al-Soud W, Rådström P. 1998. Capacity of nine thermostable DNA polymerases to mediate  
411 DNA amplification in the presence of PCR-inhibiting samples. *Appl Environ Microbiol* 64:3748–  
412 3753.
- 413 27. Kirkland P, Frost M. 2020. The impact of viral transport media on PCR assay results for the  
414 detection of nucleic acid from SARS-CoV-2. *Pathology* 52:811–814.
- 415 28. Hoorfar J, Cook N, Malorny B, Wagner M, De Medici D, Abdulmawjood A, Fach P. 2003.  
416 Making Internal Amplification Control Mandatory for Diagnostic PCR. *J Clin Microbiol*  
417 41:5835.
- 418 29. Wang D. 2016. Effect of internal primer–template mismatches on loop-mediated isothermal  
419 amplification. *Biotechnol Biotechnol Equip* 30:314–318.
- 420 30. Ayyadevara S, Thaden JJ, Shmookler Reis RJ. 2000. Discrimination of Primer 3'-Nucleotide  
421 Mismatch by Taq DNA Polymerase during Polymerase Chain Reaction. *Anal Biochem* 284:11–  
422 18.
- 423 31. Li Y, Zhou Y, Ma Y, Xu R, Jin X, Zhang C. 2019. A Mismatch-tolerant RT-LAMP Method for  
424 Molecular Diagnosis of Highly Variable Viruses. *Bio-protocol* 9:e3415.
- 425 32. GISAID. 2021. Tracking of Variants.
- 426





**C.**

SARS-COV-2 Copies	0	5	20	200	2,000
Target Detection (min)	N/A, N/A, N/A	27.3, 23.9, 23.2, 25.9	21.5, 23.2, 22.9	20.7, 20.5, 20.9	18.2, 18.3, 18.2
IAC Detection (min)	27.7, 27.5, 27.2	27.7, N/A, N/A, 27.9	N/A, N/A, 29.9	N/A, N/A, N/A	N/A, N/A, N/A



**B.**

	LAMP Replicate 1	LAMP Replicate 1
Positive >30 copies	21/21	21/21
Positive < 30 copies	6/9	5/9
Sensitivity	90%	87%
Negative	60/60	60/60
Specificity	100%	100%